

DETERMINING THE CUE TO WHICH SWIMMING ZOOPLANKTON RESPOND: ACCELERATION VERSUS SHEAR

Marek Stastna¹, Justin Shaw¹, Michael Waite¹ and Divya Lala²

¹Department of Applied Mathematics
University of Waterloo, Waterloo, Ontario, N2L 3G1, Canada

²Department of Applied Mathematics
Queen's University, Kingston, Ontario, K7L 3N6, Canada

Abstract. Flow in simple geometries has been used to characterize the material properties of non-Newtonian fluids for more than a half century. This systematic study has led to classes of rheological models that range from rigorous to phenomenological, but all include a testable set of hypotheses to discriminate between them in a rational manner. In contrast, models of the locomotion of simple organisms such as zooplankton are generally ad hoc and tested through the use of similarly ad hoc techniques. At the population level measurement is often indirect (e.g. acoustics). In this contribution we develop a simple example of an unsteady flow that is realizable in the laboratory and yields a qualitatively similar response, including limit cycles, for both shear triggered and acceleration triggered flee response. We present some very simple discrimination experiments that unambiguously determine whether a given zooplankton species exhibits shear or acceleration triggered response. Finally we demonstrate that these experiments remain robust even for more complex, and biologically more realistic models.

Keywords. rheometric flows, zooplankton locomotion, shear-triggered response, ordinary differential equations, hydrodynamics .

AMS (MOS) subject classification: 92B01

1 Introduction

According to the Greek root of the word, plankton are wanderers of, or drifters on, the world's waters. They are so numerous that their collective presence can be identified from satellite (see [9] for a recent example). Plankton exhibit a surprising range of sizes, with the subclassifications of Mesoplankton and Macroplankton (tenths of millimeters to several centimeters) being the subject of the modeling presented in this article. Phytoplankton and smaller zooplankton exhibit only limited motility, and so are passive tracers to a good approximation on the field scale. Larger zooplankton exhibit a variety of strong and complex swimming behaviors, some of which are

triggered by the plankton's reaction to something in its environment (e.g. fluid motion that indicates the approach of a predator). Effects of swimming must thus be considered if a realistic description is to be achieved. A more complete discussion can be found in many textbooks, for example [6].

Since plankton spend their lives immersed in moving water, any model of their behavior must account, at least to some extent, for the motion of the ambient fluid. Figure 1 shows a diagram of a hierarchy of models of fluid motion and plankton swimming. At the top of the hierarchy is a fully two way coupled Navier Stokes model with plankton swimming that modifies the fluid flow around it. The authors are not aware of any existing software capable of this sort of coupling. Even if it were available it is quite likely that it would be both numerically expensive, and yield so much data that one of the simplified models in the hierarchy shown in Figure 1 would be a more effective tool in exploring and understanding possible behaviors. Coupled models in the literature tend to begin with a hydrodynamic model and add a simple swimming model to a Lagrangian particle component of the hydrodynamic model [11]. This was the approach taken in [12], where linear internal waves advected plankton whose swimming was modeled as a fluid particle moving according to a biased random walk. The motion of the plankton had no effect on the hydrodynamics implying that model coupling was one way. Using a model second from the bottom of the hierarchy depicted in Figure 1, the authors found that the mechanisms of settling, a "freezing" in high shear, and biased swimming towards a preferred light level were sufficient to explain *in situ* measurements of perturbed plankton layers. So while the most sophisticated models include all mechanisms, simpler models can illuminate which of those mechanisms are important in reproducing observations.

Plankton are generally found in the near surface layer of the ocean and freshwater bodies. Motions that might affect plankton include surface waves and the currents they induce, internal waves including those with much longer horizontal length scales than surface waves, turbulent patches due to shear instability or internal wave breaking, and eddies that may carry water with very different temperature and salinity characteristics from the ambient fluid [6]. In the setting of fjords, a recent study has theorized that plankton interact with the turbulence formed due to a bottom boundary layer and its separation from the seabed [4]. The swimming behaviors of organisms on the same scale as Mesoplankton have been documented to be altered by the presence of turbulence [2]. In that paper, the authors argue that the reaction to a turbulent environment provides an explanation for the earlier observation that response to light varied with larvae age. Moreover, sinking behavior would allow the organisms to control their dispersal, something corroborated by the numerical study of Chesapeake Bay in [10]. While shear is often cited as a primary trigger for swimming behavior in a turbulent environment (for example in [4]), swimming behaviour could be triggered by many flow properties: dissipation rate, shear or acceleration. In [1] the authors discuss several possible triggers for plankton, finding similar correlations for several

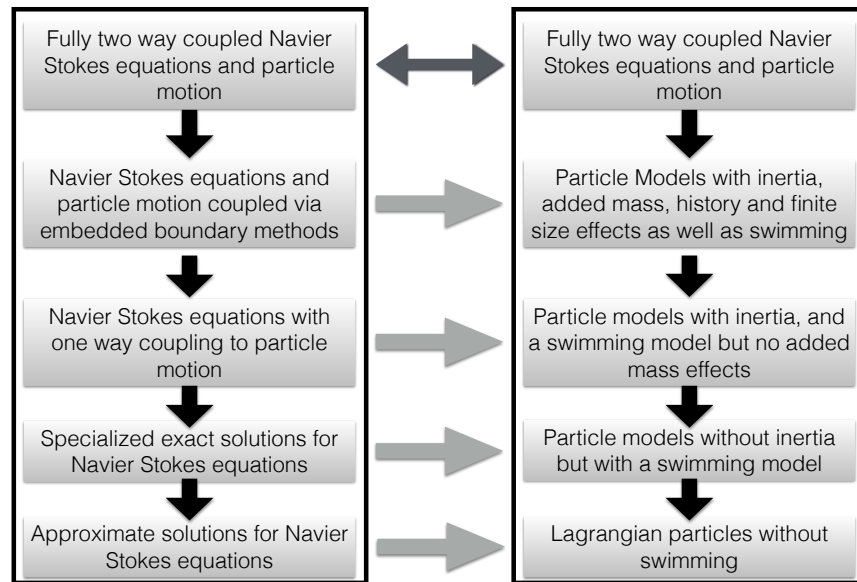


Figure 1: Schematic of the hierarchy of Navier-Stokes equation based fluid mechanics models and swimming plankton models. The left column shows the hierarchy for the fluid motions and the right column is the hierarchy for the particle models. The grey arrows indicate one way coupling and the double ended arrow indicates two way coupling. Within the columns black arrows indicate a simplification, a reduction in complexity.

different variables (see their Figure 2). At the same time it has been argued in [5] that there is a need for toy models in turbulence–plankton studies. This article argued for consideration of the Burgers vortex as a schematic representation of a local patch of turbulent fluid, but did not provide a clear assessment of different plankton swimming behaviors.

We are not the first to draw analogies with continuum mechanics in formulating models of plankton locomotion. In [7], the authors discuss deformation from a general point of view, but focus only on the classical low Reynolds number flow past a sphere solution. Nevertheless, the article discusses a broad scope of biological behaviors, including ambush feeding. In the companion paper [8] the authors focus on a particular copepod species, *Acartia tonsa* and explore a variety of simple flows and devices that have been used to explore the swimming response (see their Figure 1 for details). While these simple flows, and the response to them, provide a useful survey of experimental techniques, the conclusions give no clear delineation as to what aspect of the flow a particular organism is responding to when deciding whether to swim or not.

In order to determine whether shear or acceleration is the flow parameter inducing an escape response, we base our explorations on a flow which has both, is experimentally realizable, and which is an exact solution of the Navier-Stokes equations. The latter means that we are able to use relatively simple analytical expression for finite amplitude flows without approximation. This choice of flow has allowed us to design experiments which could determine which of these two flow parameters a given species of plankton respond to. Simple flow configurations have a long history of use in materials characterization, having the advantage of well known bounds on ranges of applicability. In particular, variants of simple shear are used in a variety of so-called rheometric flows to determine physical parameters in non-Newtonian materials (e.g. shear thinning viscosity). The flee responses discussed in [8] are generally thought to be in a direction away from the cue (see also [4]). In our chosen flow both acceleration and shear increase exponentially with depth, and so the swimming behaviors we consider are that of an upward directed flee response when local shear or local acceleration surpasses a certain critical value. We demonstrate that this response produces limit cycles which can be used to determine which of shear or acceleration are being responded to. In our conception, the simple experiments we propose would be carried out first, followed with detailed study of more complex situations including competition between response to flow and feeding.

In order to keep a consistent notation throughout the results, and because many of the conclusions we draw are equally relevant for either zooplankton or the larval stage of larger organisms, we will refer to a “particle”, or several “particles”. We return to the biologically relevant terminology in the final section. The remainder of the paper is organized as follows. The Methods section outlines the basic flow, and the tools to unambiguously characterize the shear and acceleration fields in the flow, then continues to discuss La-

granular particle models relevant for small particles. The Results consider shear triggered response due to a single driving frequency first. The acceleration triggered response is contrasted with the shear triggered response next, and a set of experiments to discriminate between the two types of trigger is proposed. Finally a more biologically realistic model is outlined, and the previously proposed experiments are reconsidered, with the goal of determining which discrimination techniques are robust when the complexity of the swimming model is increased. The article concludes with a discussion of the general conclusions and possible avenues for future work.

2 Methods

We consider the fluid motion to be given by the solution of the oscillating plate, or Stokes' second problem: the motion of a constant density, viscous fluid which occupies the upper half space overlying an oscillating plate. The motion of the plate is given by

$$u_{\text{plate}}(t) = U_0 \cos(\omega t). \quad (1)$$

The governing Navier–Stokes equations linearize geometrically in this case (or in other words without approximation) yielding the heat equation for the horizontal component of velocity

$$u_t = \nu u_{zz} \quad (2)$$

which is easily solved to give

$$u(z, t) = U_0 \cos(\omega t - mz) \exp(-mz), \quad (3)$$

while the vertical component is zero. Here

$$m = \sqrt{\frac{\omega}{2\nu}}. \quad (4)$$

where ν is the kinematic viscosity. It can be seen that the vertical decay scale of motion ($L_d = 1/m$) and vertical period of oscillation ($L_o = 2\pi/m$) scale with the square root of viscosity, and the square root of the period of oscillation $T_p = 2\pi/\omega$. Both higher viscosity and slower oscillations of the plate increase penetration of the oscillations into the fluid. For our simulations we fixed the viscosity to be that of seawater.

Results are presented in dimensionless form, scaling velocities by the velocity of the plate, lengths by the initial particle distance from the plate, and using the advective timescale derived from these two quantities. Similarly, the typical value of shear is derived from these quantities and is an upper bound on shear in the system since the amplitude of fluid motion decays as one moves away from the plate. Many representative values of parameters were explored, with values employed for the Results section listed in Table 1.

In general, as outlined in [12], quantifying shear in fluid requires consideration of the second invariant of the rate of strain tensor ([3]). However, with only one non-zero component of velocity the second invariant of the rate of strain tensor reduces to a function of simple shear, given by

$$\frac{\partial u}{\partial z}(z, t) = -U_0 m \exp(-mz) [\sin(\omega t - mz) - \cos(\omega t - mz)]. \quad (5)$$

Using trigonometric identities and (4) this expression may be rewritten as

$$\frac{\partial u}{\partial z}(z, t) = -U_0 \sqrt{\frac{\omega}{\nu}} \exp(-mz) \sin\left(\omega t - mz - \frac{\pi}{4}\right), \quad (6)$$

The acceleration takes a similar form, namely

$$\frac{\partial u}{\partial t}(z, t) = -U_0 \omega \exp(-mz) \sin(\omega t - mz), \quad (7)$$

Both the shear and the acceleration experience an exponential increase of shear near the plate ($z = 0$). In the absence of inertia the motion of the particles can be expressed in the general form as a modified path line equation

$$\frac{d\vec{x}}{dt} = \vec{u}_{\text{fluid}}(x(t), z(t), t) + \vec{u}_{\text{particle}}(x(t), z(t), t) \quad (8)$$

which for our situation simplifies to

$$\frac{d\vec{x}}{dt} = [u(z(t), t), 0] + [0, w_{\text{sink}} + H(|u_z(z(t), t)| - u_z^{\text{critical}})w_{\text{swim}}], \quad (9)$$

with an analogous expression for acceleration triggered flow. We have chosen w_{sink} to be a constant and have modeled the triggered response using a Heaviside function: if the value of the flow parameter is higher than the critical value u_z^{critical} the particles swim up. The results were found to be insensitive to the choice of critical value, so they were chosen arbitrarily. The threshold value will be determined at the same time as the relevant biological cue in the experiments outlined here. Also note that this model is an example of one that is second from the bottom of the particle model hierarchy in Figure 1.

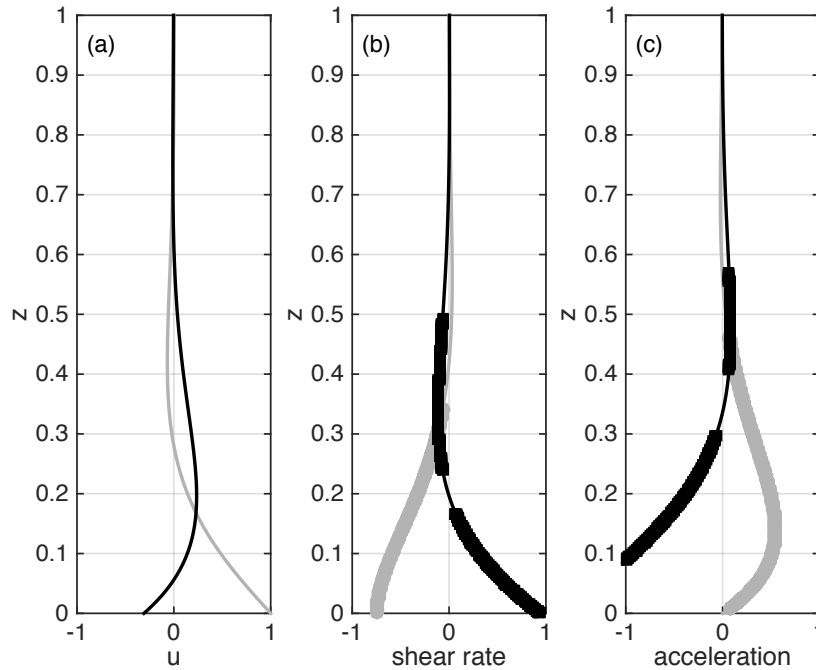


Figure 2: Schematic of the solution to the Stokes third problem. (a) the velocity versus height at two different times, (b) the shear versus height at the same two times, (c) the acceleration versus height at the same two times. The locations above a critical shear are marked with thick symbols. Note the disconnected region of high shear in the two black curves.

A sample solution of the fluid motion is shown in Figure 2. Panel a) shows the velocity field at two different times. The exponential decay of the motion away from the plate can be clearly seen. A critical shear value and a critical acceleration value were chosen. Panel b) shows the shear profile at two different times with large symbols indicating the z values at which a critical value is surpassed. Panel (c) repeats this for the acceleration profile. It is particularly interesting that for both curves shown in black there is a small sub-critical region below the uppermost super-critical region. This sub-critical region breaks up the two large regions where the critical value is surpassed, and implies that the pattern of triggered swimming exhibits a non-trivial spatiotemporal pattern.

3 Results

3.1 Shear Triggered Response

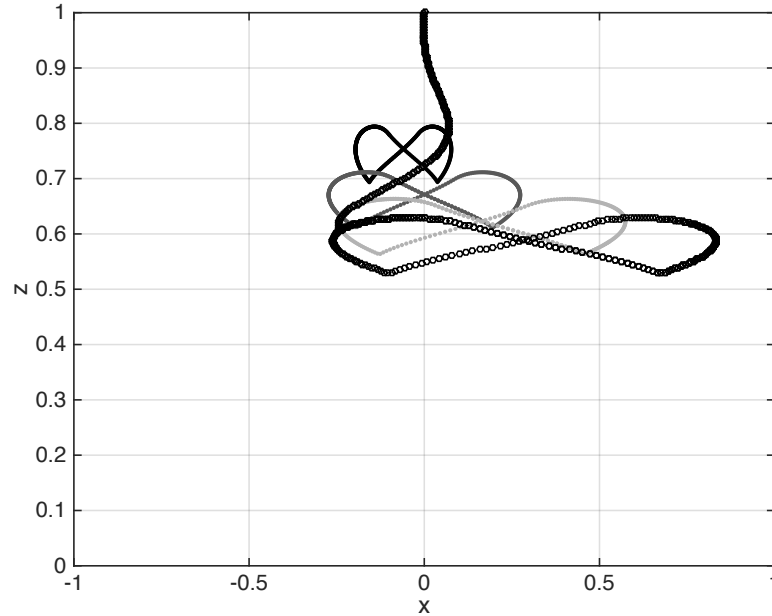


Figure 3: Sample limit cycles for the swimming particle at different critical shear values. x and z are scaled by the height of the initial position. Critical shear as a multiple of the default: 1 (black), 2 (dark grey), 3 (light grey), 4 (black symbols).

We begin by considering examples of shear triggered upward swimming for different critical shear values. Figure 3 shows four sample trajectories with increasing critical shear. A limit cycle is immediately evident in all cases, and is the result of a different balance of mechanisms in the horizontal (x) and vertical (z) directions. The horizontal motion is due to the direct influence of the fluid flow on the motion of the particle, the vertical motion is a result of the indirect influence of the flow triggering the swimming behavior to counteract the downward sinking. A necessary condition for the existence of the limit cycle in this simplest model is that the upward swimming must be strong enough to overcome the downward sinking. When this condition is not met the particle continues to sink, albeit at a reduced rate, eventually settling at the level of the plate. It can be seen that as the particles fall closer to the oscillating plate prior to their swimming being triggered, their

horizontal excursions increase while the vertical extent of the limit cycle remains essentially unchanged. This is a result of the exponential decay of the solution in the z direction.

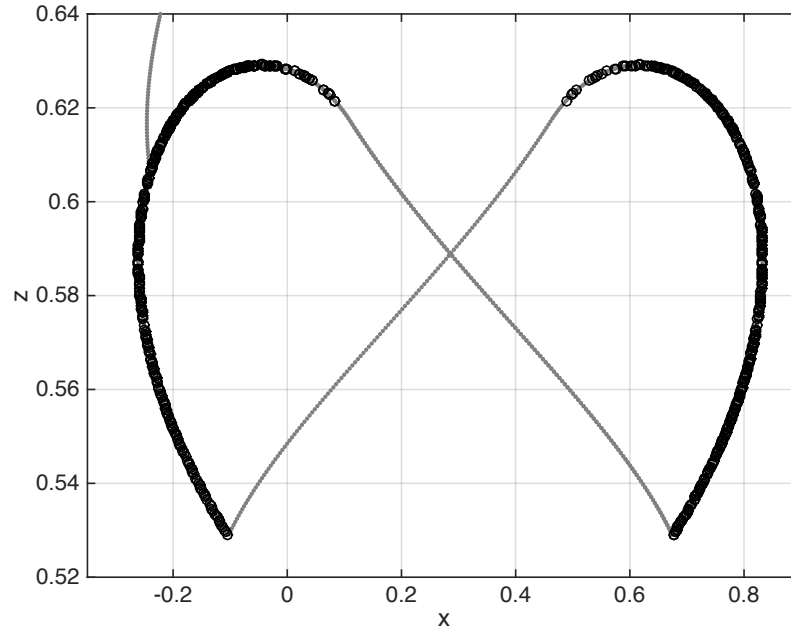


Figure 4: Sample limit cycle corresponding to case 4 in Figure 3. Output times at which swimming is ‘On’ are indicated by large black circles.

In Figure 4 we show the largest limit cycle from Figure 3 in grey. Superimposed on the path the particle follows are large circles which indicate all output times at which swimming is active or ‘On’. It is clear that the flanks of the limit cycle correspond to regions of consistent swimming. Near the top of the limit cycle the particle reaches a region of phase space in which swimming takes it out of the region where shear is high enough to trigger swimming. The particle drops and quickly reaches a region of higher shear due to the exponential behavior of the shear profile, and swimming is triggered again. The process is repeated multiple times, until the oscillation leads to a portion of the cycle where shear is sufficiently reduced so that no further swimming occurs.

3.2 Acceleration Triggered Response

Since the acceleration field has a similar form to the shear we anticipate many of the features of the previous subsection, including limit cycle behavior, will be reproduced. However, the acceleration has both a different amplitude and

a phase shift from the shear field and hence the shape of the resulting limit cycle is quite different. Figure 5 shows four sample limit cycles corresponding to different critical acceleration values. By comparing to Figure 3 it can be seen that in the acceleration case the limit cycle is ‘bowl-like’, as opposed to ‘butterfly-like’ as in Figure 3. Figure 6 demonstrates that this qualitative change in shape is due to the fact that the swimming occurs during the inner portion of the limit cycle, in spatiotemporal regions during which the magnitude of velocity is small but acceleration is large.

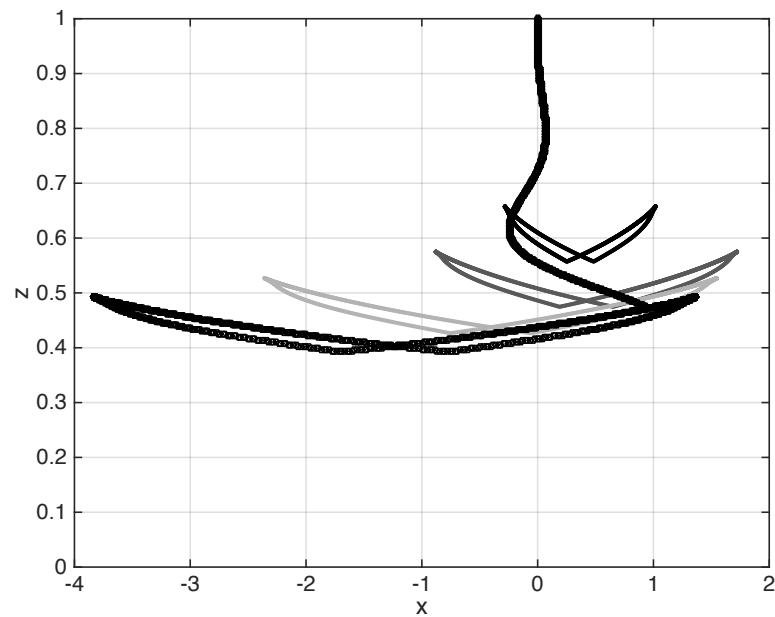


Figure 5: Sample limit cycles for the swimming particle at different critical acceleration values. x and z are scaled by the height of the initial position. Critical shear as a multiple of the default: 1 (black), 2 (dark grey), 3 (light grey), 4 (black symbols).

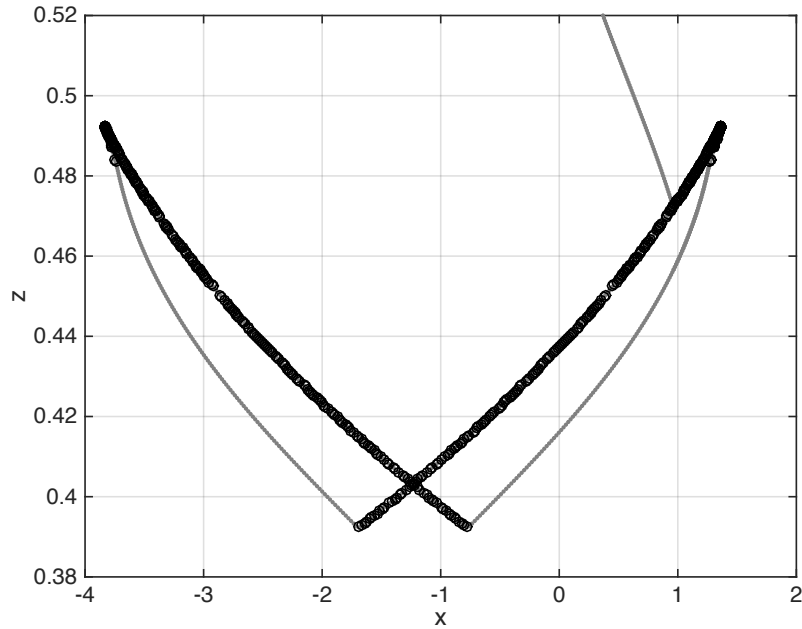


Figure 6: Sample limit cycle corresponding to case 4 in Figure 5. Output times at which swimming is ‘On’ are indicated by large black circles.

3.3 Experimental Design

We have demonstrated that for the experimentally realizable flow of a viscous fluid above an oscillating plate, the free response of a vertically dropping plankter is simply characterized for either a shear triggered or an acceleration triggered response. It remains to design an appropriate experiment that would allow for the discrimination between the two behavior types. In Figure 7, panel (a), we show the vertical position as a function of time of a particle with shear triggered swimming. Two cycles of the flow are shown, though the precise number of cycles is only clearly evident in panel (b). In this panel we show the shear (in black) and acceleration (in grey) for the same particle, again as a function of time. Both curves are scaled by their respective critical value. It is immediately evident that the shear remains very close to the critical value during the period in which the particle is swimming. In contrast the acceleration nearly doubles its critical value, and varies significantly over any time segment.

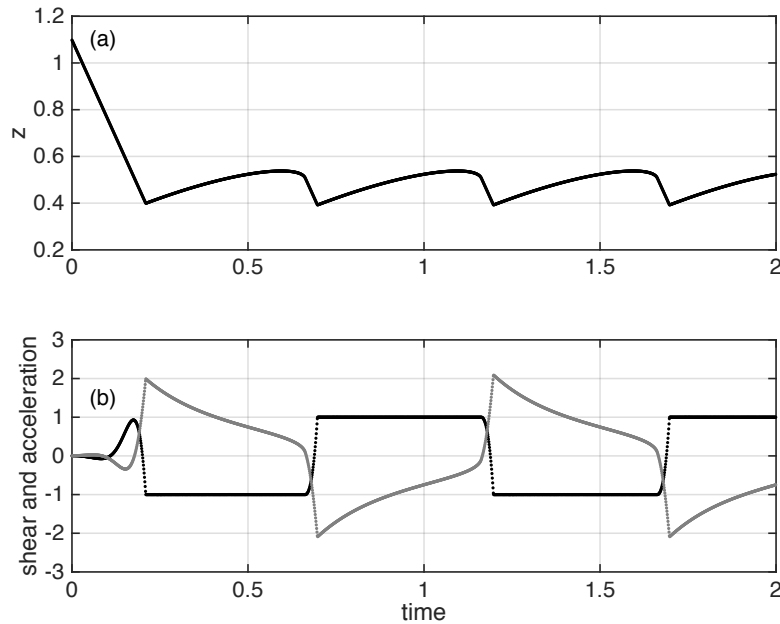


Figure 7: a) The vertical position of the particle with shear triggered swimming. b) The shear (black) and acceleration (grey) for the particle in panel (a).

Figure 8, shows the corresponding plot for acceleration triggered swimming. The particle's vertical position is shown in grey to indicate that it is acceleration triggered. It is immediately evident that in this situation it is the acceleration that plateaus near the critical value while the shear significantly exceeds the critical value and varies significantly over any time segment. Thus, an experimenter's task becomes to measure the path of a single particle over several periods of the plate's motion, and then use the analytical solution of the Navier Stokes equations to make plots corresponding to Figures 7 and 8. Based on these it should be a simple matter to decide whether acceleration or shear triggers the particle's swimming: if shear values are near constant at the particle's location it is responding to shear, and if acceleration values are near constant at the particle's location it is responding to acceleration. Additionally, this near constant value of the flow parameter is a good approximation of the critical value which induces the flee response. So then this procedure determines both which flow parameter is being responded to, and the critical value of that parameter which will induce the response.

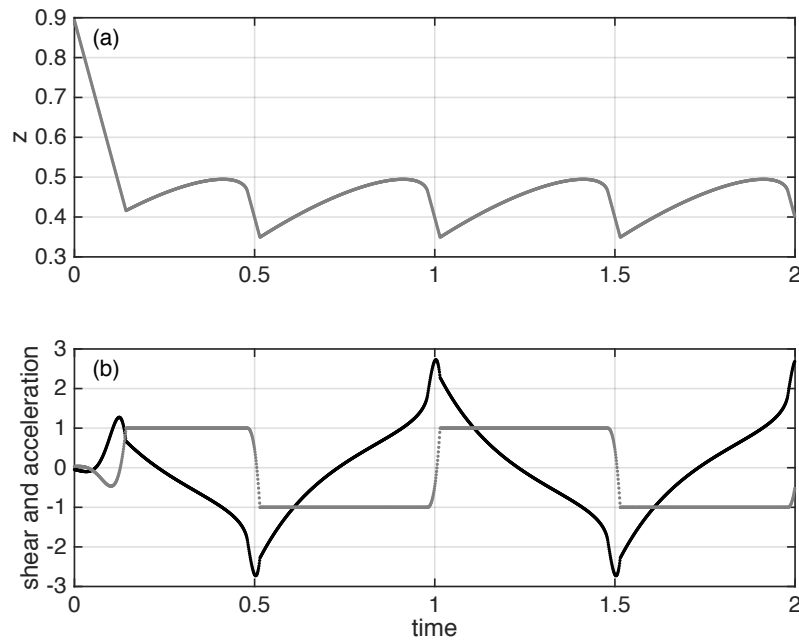


Figure 8: a) The vertical position of the particle (shown in grey to match the acceleration curve in panel b) with acceleration triggered swimming. b) The shear (black) and acceleration (grey) for the particle in panel (a).

There are several idealizations made above that may pose difficulties in the laboratory. The first is the assumption of a single individual released at a precise location. A far more realistic assumption is that of a population of individuals released in a localized area as a cloud of particles. However, even here it is not reasonable to expect that each plankter has the exact same critical value for the trigger (be it shear or acceleration). Intrinsic variation of the critical value across the population is expected. We address this concern now.

Accordingly, we have conducted numerical experiments with several different ensembles, varying the initial particle height and the critical value of shear (or acceleration) by drawing from a uniform distribution. Figure 9 shows an example of a 2000 member ensemble where the draw from the uniform distribution was over a range of 40% (25%) for the initial particle height (critical acceleration value). The Figure shows the mean (upper panel) and standard deviation (lower panel) of both the shear (black) and acceleration (grey) versus time. It can be readily seen that even accounting for the intrinsic variation of the critical value across the population and uncertainty in initial position, the standard deviation of the acceleration exhibits significant time periods where it is vanishingly small. Over the same time periods

the mean is nearly constant. Thus, by repeating the particle tracking experiment discussed above, an experimentalist can be quite confident in their prediction. However, the reader is cautioned that this result may be more subtle than it first appears since the present model idealizes biological behaviour to an extreme point, by assuming that swimming can turn on and off instantaneously.

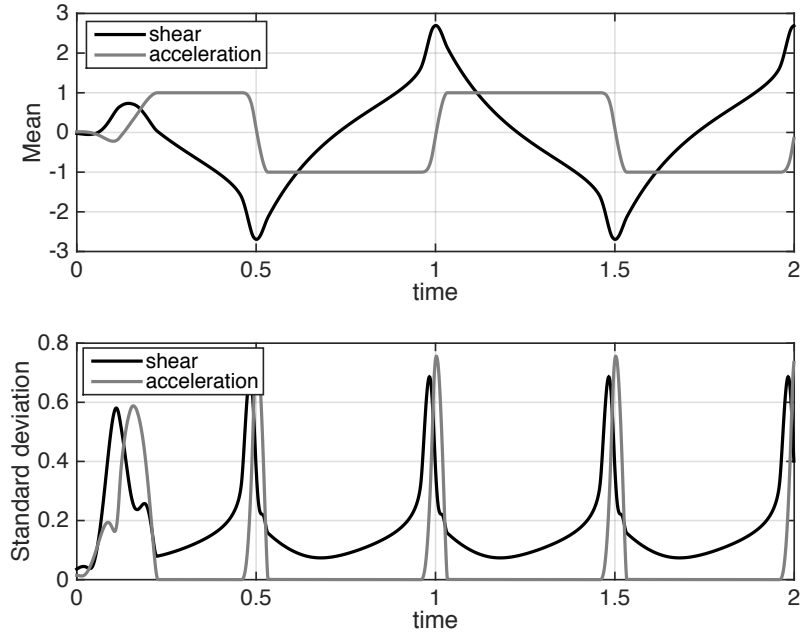


Figure 9: The mean (upper panel) and standard deviation (lower panel) of shear (black) and acceleration (grey) versus time for an ensemble of 2000 acceleration triggered particles whose initial height and critical acceleration value were chosen from a uniform distribution (details in text).

3.4 A More Biologically Reasonable Model

While the above presented results are satisfying in that they yield a non-trivial response for a very simple model, the simplifications made when modeling the swimming response may be too severe. A more complete description of swimming certainly must account for inertia, which is discussed in the accompanying paper. Additionally, from a biological standpoint it is not reasonable to assume that swimming decisions by the particle are made both instantaneously, and extremely often. These concerns can be addressed within the Lagrangian framework. While a complete treatment should consider the energetics of the organism in question, a first improvement specifies

that once swimming has begun, it must continue for a finite interval of time. In other words the particle cannot change its mind about swimming in an infinitesimal amount of time. We have found that the minimum swim time model has only a minor effect on the limit cycles. Essentially, the minimum swim time coarsens the limit cycle, as if its smooth shape in Figure 4 were approximated by many straight line segments that run at acute angles to the smooth shape.

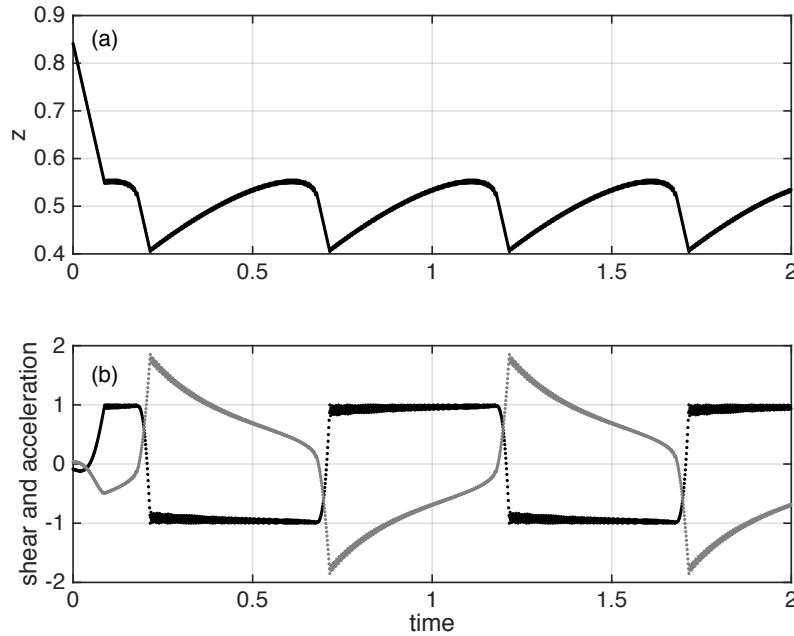


Figure 10: a) The vertical position of the particle with shear triggered swimming in the minimum swim length model. b) The shear (black) and acceleration (grey) for the particle in panel (a).

Figure 10 shows the corresponding figure to Figure 7 for the case with a minimum swim time. From the upper panel it can be seen that the curve of the vertical position versus time appears to be thicker, reflecting the jagged nature of the particle path that was discussed above. This is also reflected in the shear and acceleration curves, shown in the lower panel. It can be seen that for a single particle the ability to discriminate between a shear triggered and acceleration triggered response is maintained, since only the shear curve is seen to have nearly constant regions. However, the minimum swimming model does have an unexpected consequence as far as the bulk properties of the ensemble are concerned.

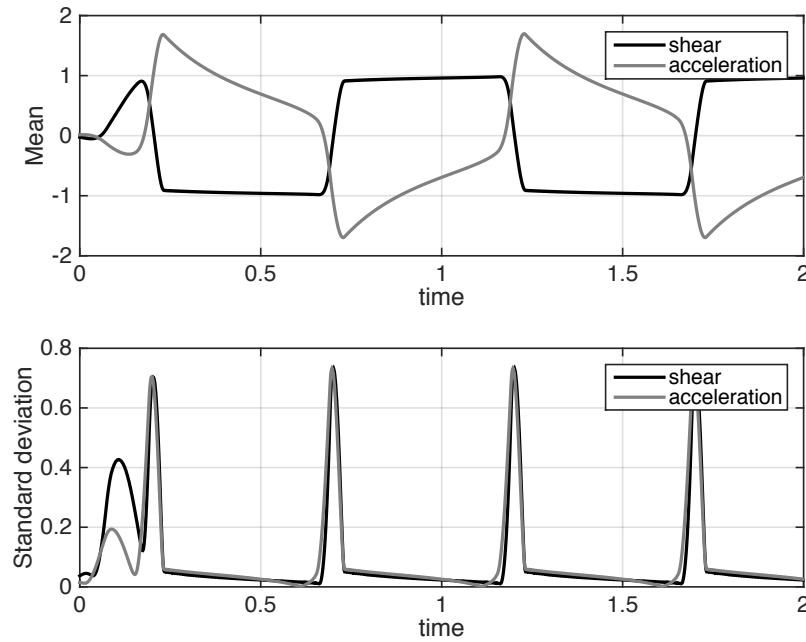


Figure 11: The mean (upper panel) and standard deviation (lower panel) of shear (black) and acceleration (grey) versus time for an ensemble of 2000 shear triggered particles with minimum swim time whose initial height and critical acceleration value were chosen from a uniform distribution (details in text).

Figure 11 shows the corresponding figure to Figure 9. It can be seen that the upper panels, which show the mean, are fairly similar. However, the lower panel showing the standard deviation is qualitatively different. The standard deviation of the shear no longer falls to zero over the nearly constant region. This is due to the ‘detuning’ of the onset of swimming between ensemble members, and suggests that any experiment based on ensemble results should consider the mean and not the standard deviation of this ensemble.

4 Conclusions

We have demonstrated that the simple laboratory situation of a large oscillating plate may be used to unambiguously discriminate between shear triggered and acceleration triggered swimming behaviour in zooplankton. The particular expression of the swimming behaviour is the formation of limit cycles in the particle position. This is due to the fact that the fluid motion only serves to move the zooplankton in the horizontal direction while the swimming,

when triggered, serves to counteract the sinking of the plankton.

The discrimination procedure is most clear when an experimentalist is able to effectively track a single individual. The basic procedure, when the path of a single plankter can be measured, is to use the analytical solution of the Navier-Stokes equations to plot the shear and acceleration as a function of time. The variable that corresponds to the trigger exhibits extended periods during which it is nearly constant. Moreover, this constant provides an estimate of the critical value of the trigger. For situations in which only the ensemble mean may be measured, we have shown that the same discrimination procedure is effective, though the critical value of the trigger will no longer be known exactly. Indeed we were able to demonstrate the efficacy of this method even when the complexity of the swimming model was increased to include a finite swimming time. In this case we found that the ensemble standard deviation versus time curves were more complex, implying that they could not be used for discrimination experiments. In contrast when ensemble properties can be measured, the ensemble mean still allows for accurate discrimination between behaviors.

Standardized experiments like those presented here could allow experimental biologists to catalogue plankton responses and their associated critical values the way that materials scientists catalogue, for example, tensile strength values. This would have enormous advantages in assisting subsequent numerical experiments. Not knowing which flow parameter is triggering the response means running an experiment requires the assumption of an unproven response. Not knowing the critical value of that parameter that triggers the response is computationally expensive because multiple critical values will need to be tested in order to establish stability of simulated phenomena across a spectrum of possible unknown values. Both of these difficulties were encountered and overcome in [12] by theorizing the response, modelling the dynamics, and comparing to acoustic data. So while it is possible to produce results without detailed knowledge of both the response and the critical value, more experiments could be run with greater confidence if both were available.

Future work could consider a number of different avenues. First of all, the analogy with rheological tests could be taken further by considering a cylindrical plate that moves in a torsional manner. This situation has the attraction that a large shear may be created even though the experimental apparatus remains fixed in size. Second, some of the more extreme simplifications in the model could be replaced with more sophisticated approximations. In particular, the swimming direction could be drawn from a distribution of directions, as opposed to assuming it is purely away from the high shear or acceleration region. Finally, a numerical model could be used to probe the high Reynolds number regime in which the oscillating flow transitions to turbulence. While this would be a considerable increase in model complexity and computational cost, it would provide information on what is thought to be the relevant fluid mechanical regime in the natural environment.

5 Acknowledgements

This work was supported by the Natural Sciences and Engineering Research Council of Canada through Discovery Grant RGPIN-311844-37157 to MS and RGPIN-386456-2010 to MW. Insightful referee comments helped improve the manuscript's clarity.

References

- [1] Fuchs, H.L. and DiBacco, C., Mussel larval responses to turbulence are unaltered by larval age or light conditions. *Limnology & Oceanography: Fluids & Environments*, 1:120–134, 2011.
- [2] Fuchs, H.L., Hunter, E.J., Schmitt, E.L. and Guazzo, R.A., Active downward propulsion by oyster larvae in turbulence. *Journal of Experimental Biology*, 216(8):1458–69, 2013.
- [3] Fung, Y.C., *A First Course in Continuum Mechanics*. Prentice-Hall, 3rd edition, 1993.
- [4] Ianson, D., Allen, S.E., MacKas, D.L., Trevorrow, M.V. and Benfield, M.C., Response of *Euphausia pacifica* to small-scale shear in turbulent flow over a sill in a fjord. *Journal of Plankton Research*, 33(11):1679–1695, 2011.
- [5] Jumars, P.A., Trowbridge, J.H., Boss, E. and Karp-Boss, L., Turbulence-plankton interactions: A new cartoon. *Marine Ecology*, 30(2):133–150, 2009.
- [6] Kennish, M.J., *Practical Handbook of Marine Science*. CRC Press, 3rd edition, 2001.
- [7] Kiørboe, T., Saiz, E. and Visser, A., Hydrodynamic signal perception in the copepod *Acartia tonsa*. *Marine Ecology Progress Series*, 179:97–111, 1999.
- [8] Kiørboe, T. and Visser, A., Predator and prey perception in copepods due to hydro-mechanical signals. *Marine Ecology Progress Series*, 179:81–95, 1999.
- [9] Navarro, G., Alvain, S., Vantrepotte, V. and Huertas, I.E., Identification of dominant phytoplankton functional types in the Mediterranean Sea based on a regionalized remote sensing approach. *Remote Sensing of Environment*, 152:557–575, 2014.
- [10] North, E.W., Schlag, Z., Hood, R.R., Li, M., Zhong, L., Gross, T. and Kennedy, V.S., Vertical swimming behavior influences the dispersal of simulated oyster larvae in a coupled particle-tracking and hydrodynamic model of Chesapeake Bay. *Marine Ecology Progress Series*, 359(Leis 2007):99–115, 2008.
- [11] Scotti, A. and Pineda, J., Plankton accumulation and transport in propagating nonlinear internal fronts. *Journal of Marine Research*, 65(1):117–145, 2007.
- [12] Shaw, J. and Stastna, M., A Model for Shear Response in Swimming Plankton. *Progress in Oceanography*, 151:1-12, 2017.

Received January 2017; revised November 2017.

email: journal@monotone.uwaterloo.ca
<http://monotone.uwaterloo.ca/~journal/>